Cech, T. R. (1987) *Science 236*, 1532–1539.
Ciesiolka, J., Marciniec, T., Dziedzic, P., Krzyzosiak, W., & Wiewidrowski, M. (1986) in *Biophosphates and Their Analogues Synthesis, Structure, Metabolism and Activity* (Bruzik, K. S., & Stec, W. J., Eds.) pp 409–414, Elsevier, Amsterdam.
Davenloo, P., Sprinzl, M., Watanabe, K., Albani, M., & Kersten, H. (1979) *Nucleic Acids Res. 6*, 1571–1581.
Dirheimer, G., Ebel, J. P., Bonnet, J., Gangloff, J., Keith, G., Krebs, B., Kuntzel, B., Roy, J., Weissenbach, J., & Werner, C. (1972) *Biochimie 54*, 127–144.
England, T. E., & Uhlenbeck, O. C. (1978) *Nature 275*, 5680.
Epstein, L. M., & Gall, J. G. (1987) *Cell 48*, 535–543.
Farkas, W. (1968) *Biochim. Biophys. Acta 155*, 401–409.
Forster, A., & Symons, R. (1987) *Cell 50*, 9–16.
Hall, K., Sampson, J., Uhlenbeck, O., & Redfield, A. (1989) *Biochemistry 28*, 5794–5801.
Hutchins, C., Rathjen, P., Forster, A., & Symons, R. (1986) *Nucleic Acids Res. 14*, 3627–3640.
Jack, A., Ladner, J. E., Rhodes, D., Brown, R. S., & Klug, A. (1977) *J. Mol. Biol. 111*, 315–328.
Krzyzosiak, W. J., Marciniec, T., Wiewiorowski, M., Romby, P., Ebel, J. P., & Giegé (1988) *Biochemistry 27*, 5771–5777.
Kuo, M., Sharmeen, L., & Dinter-Gottlieb, G. (1988) *J. Virol. 62*, 4439–4444.
Levitt, M. (1969) *Nature 224*, 759–763.
Moras, D., Dock, A. C., Dumas, P., Westhof, E., Romby, P., Ebel, J. P., & Giegé, R. (1986) *Proc. Natl. Acad. Sci. U.S.A. 83*, 932–936.
Potts, R., Ford, N., & Fournier, M. (1981) *Biochemistry 20*, 1653–1659.
Reilly, R. M., & RajBhandry, U. L. (1986) *J. Biol. Chem. 261*, 2928–2935.
Romby, P., Carbon, P., Westhof, E., Ehresmann, C., Ebel, J. P., Ehresmann, B., & Giegé, R. (1987) *J. Biomol. Struct. Dyn. 5*, 669.
Rordorf, B., & Kearns, D. (1976) *Biopolymers 15*, 1491–1504.
Rubin, J. R., & Sundaralingam, M. (1983) *J. Biomol. Struct. Dyn. 1*, 639–646.
Sampson, J. R., & Uhlenbeck, O. (1988) *Proc. Natl. Acad. Sci. U.S.A. 85*, 1033.
Sampson, J. R., Sullivan, F. X., Behlen, L. S., DiRenzo, A. B., & Uhlenbeck, O. C. (1987) *Cold Spring Harbor Symp. Quant. Biol. 52*, 267–277.
Sampson, J. R., DiRenzo, A. B., Behlen, L. S., & Uhlenbeck, O. C. (1989) *Science 243*, 1363–1366.
Sampson, J. R., DiRenzo, A. B., Behlen, L. S., & Uhlenbeck, O. C. (1990) *Biochemistry* (following paper in this issue).
Sundaralingam, M., Rubin, J. R., & Cannon, J. F. (1984) *Int. J. Quantum Chem., Quantum Biol. Symp. 11*, 355–366.
Sussman, J. L., & Podjarny, A. D. (1983) *Acta Crystallogr. 39B*, 495–505.
Uhlenbeck, O. C. (1987) *Nature 328*, 596.
Werner, C., Krebs, B., Keith, G., & Dirheimer, G. (1976) *Biochim. Biophys. Acta 432*, 161–175.
Westhof, E., & Sundaralingam, M. (1986) *Biochemistry 25*, 4868–4878.
Yu & Fritchie (1975) *J. Chem. Soc., Dalton Trans.*, 377.

Role of the Tertiary Nucleotides in the Interaction of Yeast Phenylalanine tRNA with Its Cognate Synthetase†

Jeffrey R. Sampson, Anthony B. DiRenzo, Linda S. Behlen, and Olke C. Uhlenbeck*
Department of Chemistry and Biochemistry, University of Colorado, Boulder, Colorado 80309-0215
Received August 4, 1989; Revised Manuscript Received October 23, 1989

ABSTRACT: In vitro transcription by T7 RNA polymerase was used to prepare 32 different mutations in the 21 nucleotides that participate in the 9 tertiary base pairs or triples of yeast $tRNA^{Phe}$. The mutations were designed either to disrupt the tertiary interaction or to change the sequence without disrupting the structure by transplanting tertiary interactions present in other tRNAs. Steady-state aminoacylation kinetics with purified yeast phenylalanyl synthetase revealed little change in reaction rate as long as a tertiary interaction was maintained. This suggests that the tertiary nucleotides only contribute to the folding of $tRNA^{Phe}$ and do not participate directly in sequence-specific interaction with the synthetase.

The crystal structure of yeast $tRNA^{Phe}$ contains nine tertiary interactions that contribute to the folded structure of the tRNA (Figure 1) (Robertus et al., 1974; Kim et al., 1974). With one exception, these tertiary interactions involve nonstandard base pairs and in three cases involve interaction between three nucleotides (Figure 2). A comparison of more than 200 available nonmitochondrial tRNA sequences reveals that of the 21 nucleotides involved in these interactions 9 are completely conserved and 9 more are semiconserved as either a purine or pyrimidine (Grosjean et al., 1982). The observed covariance of the semiconserved nucleotides in other tRNA sequences suggested that many tertiary interactions can be replaced by other nucleotides with only minimal alterations of the phosphodiester backbone (Robertus et al., 1974; Klug et al., 1974; Kim, 1976). The crystal structures of yeast $tRNA^{Asp}$, yeast $tRNA^{Metf}$, and *Escherichia coli* $tRNA^{Metf}$ confirmed several of these alternate tertiary motifs (Westhof et al., 1985; Schevitz et al., 1979; Woo et al., 1980). In addition to their structural role, it has been proposed that several of the tertiary nucleotides are important for recognition by various enzymes that interact with tRNA. For example, the conserved TΨC sequence has been proposed to interact with the ribosome (Erdmann et al., 1973), and a subset of the conserved nucleotides in yeast $tRNA^{Phe}$ and $tRNA^{Leu}$ precursors may be specifically recognized by the tRNA splicing apparatus (Reyes & Abelson, 1988; Mattoccia et al., 1988).

† Supported by the National Institutes of Health (GM 37552).

0006-2960/90/0429-2523$02.50/0

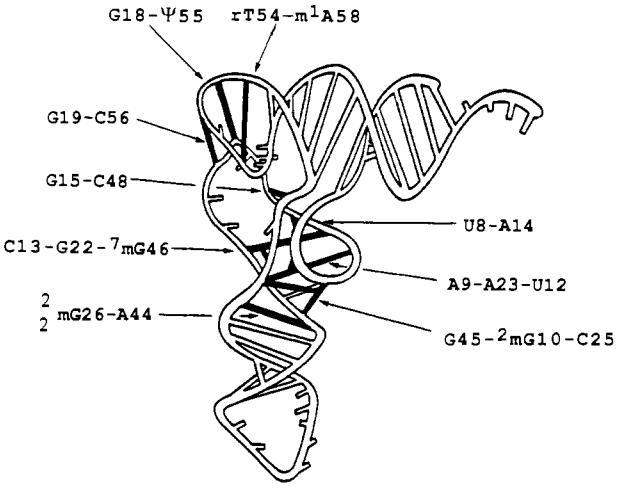

FIGURE 1: Tertiary structure of yeast $tRNA^{Phe}$ with location and identity of the nine tertiary interactions.

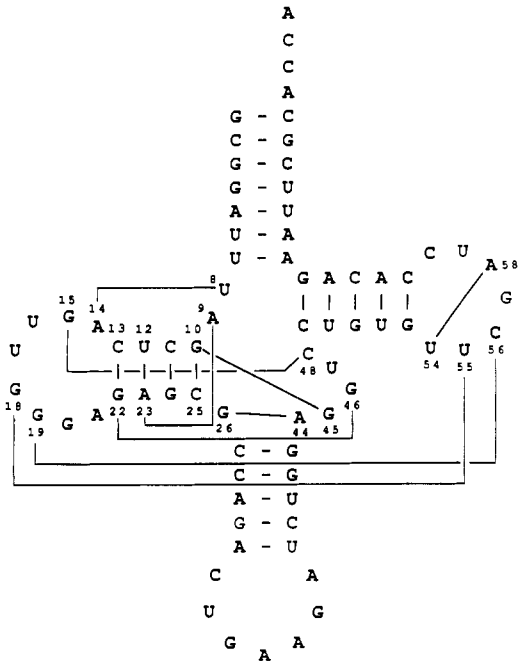

FIGURE 2: Yeast $tRNA^{Phe}$ sequence with the nucleotides involved in tertiary interactions numbered and joined by lines.

The goal of the work presented here is to evaluate the role the tertiary interactions in yeast $tRNA^{Phe}$ play in the aminoacylation reaction with the cognate yeast phenylalanyl-tRNA synthetase (FRS). At least three different, nonexclusive roles for these nucleotides can be envisaged. First, it is possible that some of the semiconserved nucleotides could contact the enzyme and aid in the discrimination process. Although none of the 21 tertiary nucleotides are unique to $tRNA^{Phe}$, a combination of tertiary nucleotides and other single- or double-stranded residues could be used by FRS to recognize $tRNA^{Phe}$. For example, the G26–A44 tertiary pair could help FRS discriminate $tRNA^{Phe}$ from the 50% of tRNAs in yeast that do not have this same interaction.

In a second potential role, the tertiary nucleotides could serve as sites of contact with FRS that are not discriminatory but contribute to the affinity of tRNA for the enzyme. Such contacts could explain the substantial affinity of many noncognate tRNAs for FRS (Rigler et al., 1976; Roe et al., 1973). While the completely conserved nucleotides may be the best candidates for making such nondiscriminatory contacts, semiconserved nucleotides could participate as well. For example, FRS could contact the N7 of G15 and thus be able to interact with all yeast tRNAs at this conserved purine.

Finally, it is possible that FRS does not interact directly with any of the tertiary nucleotides but requires their presence to maintain the folding of the molecule. If this were the case, each of the semiconserved tertiary interactions of $tRNA^{Phe}$ could be substituted with one of the corresponding interactions found in other tRNAs. This view is supported by the fact that *Schizosaccharomyces pombe* $tRNA^{Phe}$ has two tertiary interactions which differ from yeast $tRNA^{Phe}$ and remains a good substrate for FRS (McCutchen et al., 1978). Alternatively, if the aminoacylation mechanism involves a conformational change that disrupts one or more tertiary interactions, certain structurally conservative substitutions might not be tolerated since they could not participate in the conformational change.

Using a combination of a specific gene synthesis and in vitro transcription by T7 RNA polymerase, it is possible to synthesize an RNA having the sequence of $tRNA^{Phe}$ without any of the modified nucleotides (Sampson & Uhlenbeck, 1988). Since this tRNA transcript is a good substrate for FRS, mutant tRNAs with nucleotide substitutions at any desired position can be prepared for structure–function studies. We have exploited this technology to identify five single-stranded residues that are important for recognition by FRS (Sampson et al., 1989). When *E. coli* $tRNA^{Phe}$ and three noncognate yeast tRNAs were modified to contain these five nucleotides, they become efficient substrates for FRS. Here, we use the same methodology to systematically substitute nucleotides involved in tertiary interactions. While most mutants were designed to maintain the tertiary stability of the tRNA, a few were made to disrupt a given tertiary interaction. The resulting steady-state kinetic analysis of these mutants with purified FRS makes it possible to evaluate the contribution of each of the tertiary interactions in $tRNA^{Phe}$ to the recognition process.

Materials and Methods

With the exception of p67YF33 and p67YF70, all plasmids containing the mutant tRNA genes were constructed from DNA oligonucleotides as described by Sampson and Uhlenbeck (1988). After ligation of the 6 annealed DNA oligomers, the 105 base pair product was not gel purified as before but added directly to the ligation mixture containing the *Eco*R1/*Bam*H1-digested pSP65 or pUS618, which is a derivative of pUC18 containing an upstream SP6 RNA polymerase promoter (C. Stover, unpublished results). p67YF70 and p67YF33 were constructed by taking advantage of the internal unique *Bgl*II site in the $tRNA^{Phe}$ gene. The 70 base pair *Bgl*II/*Hin*dIII restriction fragment of p67YF6 containing the 3′ half of the tRNA gene with the G46A mutation was subcloned into the 2750 base pair *Bgl*II/*Hin*dIII restriction fragment of p67YF42 containing the 5′ half of the tRNA gene with the C13U and G22A mutations to make p67YF70 (U13, A22, A46). p67YF33 was constructed in a similar fashion from p67YF27 and p67YF25. Both strands of all the mutant plasmids were sequenced in the region of the tRNA gene as described by Morin and Cech (1988).

Each mutant tRNA was transcribed in a 0.3-mL reaction mixture containing 40 mM Tris-HCl (pH 8.1), 22 mM $MgCl_2$, 1 mM spermidine, 5 mM DTT, 4.0 mM of each NTP (pH 8.0), 30 μg of *Bst*N1-digested plasmid DNA, 2 units of inorganic pyrophosphatase, and 0.1 mg/mL T7 RNA polymerase. Incubation was at 42 °C for 4 h. The tRNA transcripts were purified to single nucleotide resolution by electrophoresis on 20% polyacrylamide gel and eluted as previously described (Sampson & Uhlenbeck, 1988). The concentration of each mutant tRNA sample was determined from the absorbance

Table I: Tertiary Interactions for Nonmitochondrial Elongator tRNAs

tertiary interaction	figure	% of tRNAs
G19–C56		100[a]
G18–U55	3A	100[a]
U54–A58	4A	100[a]
U8–A14	5A	100[a]
G15–C48	6A	81[a]
A15–U48	6B	14[a]
other		6
C13–G22–G46	7A	74[a]
U13–G22–A46		10[a]
U13–G22–G46	7B	8
U13–A22–A46	7C	2
other		6
A9–A23–U12	8A	69[a]
G9–C23–G12	8D	11[a]
G9–A23–U12	8B	4
G19–G23–C12	8C	3
other		13
G45–G10–C25	9A	56[a]
U45–G10–C25	9B	19[a]
G45–G10–U25	9C	15
other		10
G26–A44	10A	50[a]
A26–G44	10B	21
A26–A44	10D	10
G26–U44	10E	3
other		16

[a] Structure present in at least one tRNA crystal structure.

at 260 nm by assuming an extinction coefficient of 5.3×10^5 M^{-1} cm^{-1}. Approximately 150–200 μg of purified tRNA was obtained from these 0.3-mL reactions.

The aminoacylation kinetics were performed in 60-μL reaction mixtures containing 30 mM Hepes–KOH (pH 7.45), 15 mM $MgCl_2$, 25 mM KCl, 10 μM [^{3}H]phenylalanine, 2.0 mM ATP, and 4 mM DTT. The tRNA samples were heated to 85 °C in 10 mM Tris-HCl and 1 mM EDTA (pH 7.0) for 3 min and slow cooled to 25 °C prior to the addition to the aminoacylation reaction mixture. K_m and k_{cat} values were obtained from an Eadie–Hofstee analysis of the initial rates using six concentrations of tRNA and an FRS concentration of 0.1 unit/mL (1 nM). The correlation coefficients for the Eadie–Hofstee plots were all 0.97 or greater, and the values of k_{cat}/K_m can be considered to be within 10% of the indicated values.

Results and Discussion

In vitro transcription was used to prepare 32 tRNA transcripts with mutations in each of the 9 tertiary interactions in yeast $tRNA^{Phe}$. Since the primary goal of this work was to establish whether FRS interacts with any of these nucleotides, most of the mutations were designed to make the smallest possible changes in the tertiary structure of the molecule. Two approaches were used to accomplish this goal. For the five semiconserved tertiary interactions, the nucleotides of a given tertiary interaction were generally replaced with nucleotides present in other tRNAs that form the same tertiary interaction. Table I lists the tertiary interactions observed for 132 nonmitochondrial elongator tRNAs with similar structures. Yeast $tRNA^{Phe}$ happens to contain all nine of the most commonly used tertiary interactions. It is likely that the groups of nucleotides present in the other tRNAs pair in a way that only minimally alters the tRNA backbone but in many cases changes the functional groups available for contact with the synthetase. Several of the tertiary interactions indicated by footnote *a* in Table I appear in the crystal structures of yeast $tRNA^{Asp}$ (Westhof et al., 1985), yeast $tRNA_f^{met}$ (Schevitz et al., 1979), and *E. coli* $tRNA^{Met}$ (Woo et al., 1980).

Table II: Aminoacylation Kinetics for $tRNA^{Phe}$ Mutants Involving Conserved Nucleotides

plasmid	tertiary interaction	figure	pmol/A_{260}	K_m (nM)	k_{cat}	k_{cat}/K_m
p67YF0	G19–C56		1400	310	(100)	(1.0)
p67YF1	G19–G56		1400	1300	90	0.21
p67YF3	C19–C56		1300	1400	80	0.17
p67YF2	C19–G56		1400	310	200	2.0
p67YF0	G18–U55	3A	1400	320	(100)	(1.0)
p67YF13	G18–C55	3B	1400	670	150	0.70
p67YF12	A18–U55	3C	1400	1200	50	0.15
p67YF14	A18–C55	3D	1300	1400	100	0.23
p67YF0	U54–A58	4A	1300	320	(100)	(1.0)
p67YF30	C54–A58	4C	1300	570	20	0.11
p67YF31	U54–G58	4D	1300	400	75	0.64
p67YF40	A54–A58	4B	1300	470	65	0.46
p67YF0	U8–A14	5A	1400	360	(100)	(1.0)
p67YF5	C8–A14	5C	1400	600	65	0.40
p67YF15	U8–G14	5D	1400	1400	80	0.20
p67YF39	A8–A14	5B	1300	660	95	0.52

The other approach to the design of $tRNA^{Phe}$ mutants employed model building. Mutations were chosen that were expected to cause minimal distortion of the backbone after they were inserted into the structure and rearranged to make reasonable hydrogen bonds to neighboring nucleotides. In some cases such design was straightforward, as in replacements of the Watson–Crick pair between G19 and C56. Often, however, more than one alternate pairing scheme could be proposed for a given mutant. Figures 3–10 show proposed tertiary interactions for many of the mutants studied in this work. Known and previously proposed arrangements were used when available. For new mutations hydrogen-bonding schemes were chosen that caused the least distortion in the phosphodiester backbone.

Aminoacylation of the mutant tRNA transcripts was carried out in a buffer containing 15 mM $MgCl_2$. Although this relatively high concentration of divalent ion will reduce the accuracy of the aminoacylation reaction (Loftfield et al., 1981), it minimizes the effect of the missing modified nucleotides (Sampson & Uhlenbeck, 1988; Hall et al., 1989). In addition, since high divalent ion concentrations will stabilize RNA folding, any destabilizing effect as a result of the mutation will be minimized. Thus, any observed changes in the aminoacylation activity are likely to be due to an alteration in the specific contact between the enzyme and the RNA. To determine the purity of each mutant tRNA, the phenylalanine acceptor activity was measured at a very high FRS concentration. As shown in Tables I and II, all mutant tRNAs could be aminoacylated to a final level of 1200–1400 pmol/A_{260}, which is consistent with the levels previously reported for both the fully modified yeast $tRNA^{Phe}$ and the wild-type $tRNA^{Phe}$ transcript (Sampson & Uhlenbeck, 1988). These experiments demonstrate that none of the mutant tRNAs fold into stable, inactive alternate conformations and thereby permit a steady-state analysis of the aminoacylation kinetics for each mutant tRNA.

The steady-state kinetics of the mutant tRNAs are given in Tables II and III for each tertiary interaction. Both k_{cat} and k_{cat}/K_m are normalized to the wild-type transcript to facilitate comparison. In general, the effects of the mutation on aminoacylation are quite small. The largest decrease in k_{cat}/K_m for a mutant designed to be structurally similar is only

Table III: Aminoacylation Kinetics of $tRNA^{Phe}$ Mutants Involving Semiconserved Nucleotides

plasmid	tertiary interaction	figure	pmol/A_{260}	K_m (nM)	k_{cat}	k_{cat}/K_m
p67YF0	G15–C48	6A	1400	320	(100)	(1.0)
p67YF11	A15–U48	6B	1300	330	160	1.6
p67YF9	A15–C48	6D	1400	380	150	1.3
p67YF10	G15–U48	6C	1300	620	90	0.46
p67YF36	G15–G48	6E	1300	2000	160	0.26
p67YF0	C13–G22–G46	7A	1400	360	(100)	(1.0)
p67YF6	C13–G22–A46	7D	1400	410	80	0.73
p67YF21	U13–G22–G46	7B	1300	330	130	1.4
p67YF42	U13–A22–G46	7E	1300	370	55	0.53
p67YF70	U13–A22–A46	7C	1300	350	120	1.2
p67YF45	C13–G22–C46	7F	1300	630	70	0.40
p67YF0	A9–A23–U12	8A	1400	340	(100)	(1.0)
p67YF7	G9–A23–U12	8B	1300	440	100	0.83
p67YF43	G9–G23–C12	8C	1300	440	95	0.81
p67YF8	G9–C23–G12	8D	1200	630	95	0.55
p67YF44	U9–A23–U12	8E	1300	610	90	0.55
p67YF0	G45–G10–C25	9A	1400	340	(100)	(1.0)
p67YF16	U45–G10–C25	9B	1300	350	100	0.95
p67YF26	G45–G10–U25	9C	1300	380	110	0.95
p67YF59	G45–C10–G25	9D	1300	580	150	0.88
p67YF0	G26–A44	10A	1400	330	(100)	(1.0)
p67YF25	G26–G44	10C	1200	210	110	1.6
p67YF27	A26–A44	10D	1400	280	100	1.2
p67YF33	A26–G44	10B	1400	240	110	1.5
p67YF41	G26–U44	10E	1300	250	100	1.3

about 2-fold. Slightly larger decreases are observed for some mutations that disrupt a tertiary interaction. These effects are less than the 10–15-fold reductions in k_{cat}/K_m seen when one of the five recognition nucleotides is changed (Bruce & Uhlenbeck, 1982; Sampson & Uhlenbeck, 1988; Sampson et al., 1989). In addition, in the course of this work we obtained several gratuitous mutations that would be expected to change the structure of the molecule more severely. Although their aminoacylation kinetics were not analyzed as carefully, it was clear that they showed much larger decreases in k_{cat}/K_m. Thus, the relatively modest changes in k_{cat}/K_m reported here are a consequence of the conservative design of the mutations tested. A discussion of the data for mutants in individual tertiary interactions follows.

The G19–C56 Tertiary Interaction. All nonmitochondrial tRNAs that have been sequenced to date have a guanosine at position 19 in the D loop and a cytidine at position 56 in the TΨC loop (Table I). The crystal structure of yeast $tRNA^{Phe}$ shows that these two nucleotides form a slightly distorted Watson–Crick base pair at the outermost corner of the folded structure and stabilize the interaction between the D loop and the TΨC loop (Figure 1). This same tertiary interaction is also present in the crystal structure for *E. coli* $tRNA^{Met\text{-}f}$. However, in the crystal structure of yeast $tRNA^{Asp}$, C56 remains stacked on the G57 and G19 has been displaced about 4 Å, thereby disrupting this base pair (Moras et al., 1983; Westhof et al., 1985). Moras et al. (1983) proposed that the loss of this tertiary interaction was due to a long-range conformational change resulting from the base pairing between the anticodon nucleotides of two adjacent tRNAs in the crystal lattice. Since FRS is known to interact with the anticodon nucleotides of yeast $tRNA^{Phe}$ (Bruce & Uhlenbeck, 1982), an alteration of the G19–C56 tertiary interaction may affect the kinetics of aminoacylation by a similar long-range conformational change.

Three mutants of the G19–C56 tertiary interaction were prepared. Model-building studies indicated that while the G19C and C56G single mutants could not form an alternative pair without greatly distorting the phosphodiester backbone, the G19C, C56G double mutant should be able to form a very similar tertiary interaction. The aminoacylation kinetic data for these mutant tRNAs are given in Table II. Both the single mutants exhibit a 5–6-fold higher K_m and a normal k_{cat} as compared to the wild-type transcript. In contrast, the double mutant which should restore the potential base pair has a normal K_m and a 2-fold greater k_{cat}. The K_m differences can most easily be understood in terms of an intact tRNA tertiary structure being required for the initial binding of the synthetase. When the base pair cannot form properly, the tRNA backbone is capable of alternate conformations which must be adapted to fit the tRNA binding site on FRS, thereby resulting in a higher K_m. The observed 5-fold decrease in the rate of specific cleavage of $tRNA^{Phe}$ by lead supports the view that the mismatched mutants have an altered tertiary structure (Sampson et al., 1988; Behlen et al., 1990). Since the lead cleavage reaction involves a region of the tRNA tertiary structure that is only about 6 Å away from the G19–C56 tertiary base pair (Brown et al., 1985), these data strongly suggest that the single mutations result in a substantial change in this region of the tRNA tertiary structure. Preliminary optical melting profiles and NMR data for the same mutant tRNAs also support this view (J. Sampson and K. Hall, unpublished results).

The virtually normal k_{cat} values for the G19C and C56G mismatch mutants suggest that once the mutant tRNA is bound to the enzyme, catalysis proceeds normally. This situation is not observed for the double mutant, however, as the k_{cat} is consistently about 2-fold higher than that of the wild-type and single mutant transcripts. Since catalysis is generally considered to be concomitant with the proposed tRNA conformational change (Riesner et al., 1976), one possible explanation for this effect is that the double mutant is able to undergo this rearrangement step faster. Alternatively, a C19–G56 base pair could invoke a particular static conformation on the tRNA which more closely resembles the active "transition state" conformation, thereby facilitating the catalytic step.

The available data therefore strongly suggest that FRS does not interact directly with specific functional groups on the G19–C56 base pair. However, the requirement for an intact pair suggests that FRS is sensitive to the structure in this region and may contact the tRNA nearby. Ethylnitrosourea footprinting studies indicate contacts between $tRNA^{Phe}$ and FRS at the nearby phosphates 56–58 (Romby et al., 1985). We have also demonstrated a nucleotide-specific contact at the nearby single-stranded G20 (Sampson & Uhlenbeck, 1988; Sampson et al., 1989).

While these results indicate a structural role for the G19–C56 tertiary base pair on FRS recognition, these two nucleotides have been implicated as sequence-specific elements for other reactions. It has been proposed that the conserved TΨC Pu in the T loop is important for the binding of tRNA on the ribosome (Erdmann, 1973). Some experimental evidence suggests that the conserved C56 is important for the recognition of the tRNA precursor by RNase P (Chris Stover, unpublished results). Perhaps the strongest evidence for a sequence-specific requirement involving the G19–C56 tertiary base pair is with the endonuclease which removes the tRNA intron. The purified yeast endonuclease is not active on the C56G mutant even when the G19C mutation is present as well, suggesting that the enzyme recognizes C56 specifically (Reyes & Abelson, 1988). A similar result has also been reported for the yeast $tRNA^{Leu3}$ gene injected into *Xenopus oocytes* (Mattoccia et al., 1988).

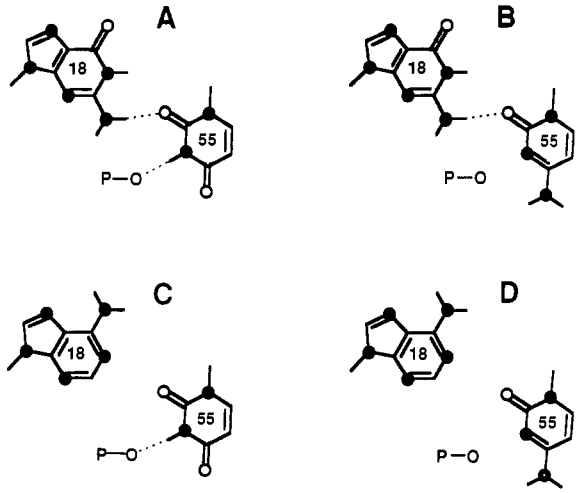

FIGURE 3: Proposed hydrogen bonding for the mutations in the conserved G18–Ψ55 pair. (A) G18–U55, (B) G18–C55, (C) A18–U55, (D) A18–C55.

The G18–Ψ55 Tertiary Interaction. In the crystal structure of yeast $tRNA^{Phe}$, the conserved nucleotides G18 and Ψ55 form a tertiary interaction which is stacked between G57 and the rT54–m1A58 tertiary interaction (Figure 1). As shown in Figure 3A, the glycosyl bonds of these two nucleotides are in a trans orientation and a single hydrogen bond is formed between the exocyclic amine of G18 and the O4 of U55. An additional hydrogen bond occurs between the imino proton of U55 and an oxygen atom of the nearby phosphate 58. Although a pseudouridine is generally conserved at position 55, both hydrogen bonds can be made with a uridine as well. It is not possible to substitute nucleotides at either position without disrupting one or both hydrogen bonds or substantially altering the phosphodiester backbone. As shown in Figure 3B,C, it is possible to maintain one equivalent hydrogen bond with either G18–C55 or A18–U55. An A18–C55 double mutant would be expected to eliminate both hydrogen bonds and therefore disrupt this tertiary interaction (Figure 3D).

The aminoacylation kinetics of the three mutations in the G18–U55 interaction reveals that both hydrogen bonds appear to be important for the optimal interaction with FRS. The K_m value for the G18A mutant, which lacks the hydrogen bond between the two loops, is greater than that for the U55C mutant, which lacks the intraloop hydrogen bond. The double mutant, lacking both hydrogen bonds, exhibits the greatest increase in K_m. Since the reduced lead cleavage rate (Behlen et al., 1990) corresponds closely to the observed increase in K_m for all three mutants, it appears that the altered tertiary structure of the mutants affects their affinity to FRS. The G18–U55 mutants also show small changes in k_{cat} as well. These differences may reflect the differential ability of these tRNAs to undergo the conformational transition suggested above. Thus, like the G19–C56 interaction, the G18–U55 interaction is essential for maintaining the correct interaction between the D and T loops necessary for recognition by FRS, but neither G18 nor U55 is likely to be involved in direct contact with the synthetase.

The U54–A58 Tertiary Interaction. In this intraloop interaction between two conserved nucleotides, a reverse Hoogsteen base pair forms in which the imino proton of rT54 is hydrogen bonded to the N7 of m1A58 and the exocyclic amine of m1A58 is hydrogen bonded to the O2 of rT54. This planar pair is stacked between G18–Ψ55 and the conserved G53–C61 base pair of the T stem and serves to stabilize the T-loop conformation (Figure 1) (Quigley & Rich, 1976).

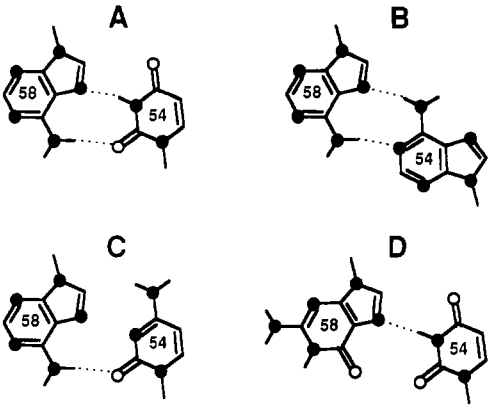

FIGURE 4: Proposed hydrogen bonding for mutations in the conserved T54–m1A58 pair. (A) U54–A58, (B) A54–A58, (C) C54A58, (D) U54–G58.

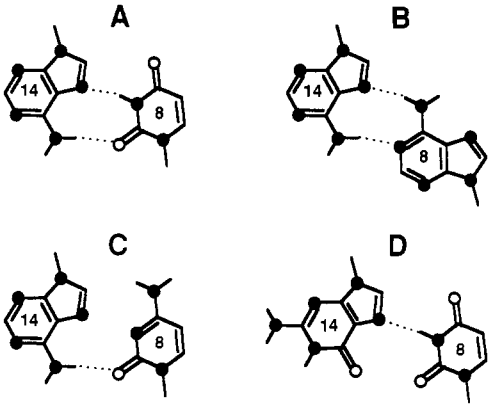

FIGURE 5: Proposed hydrogen bonding for mutations in the conserved U8–A14 pair. (A) U8–A14, (B) A8–A14, (C) C8–A14, and (D) U8–G14.

Since neither methyl group of rT54 or m1A58 is directly involved in the hydrogen bonds, it is possible to form an equivalent interaction between U54 and A58 (Figure 4A). An interesting variant of this interaction is found in many eukaryotic initiator tRNAs where an adenosine is conserved at position 54. The crystal structure of yeast $tRNA^{Metf}$ shows a similar reverse Hoogsteen base pair between A54 and A58 (Figure 4B) requiring only a minimal alteration of the phosphodiester backbone to accommodate the greater distance between the glycosidic bonds (A. Basavappa, personal communication). Model building suggests a C54–A58 could also form a tertiary base pair with one or two hydrogen bonds depending upon the exact orientation of the two nucleotides (Figure 4C). In addition, a U54–G58 could fit but would retain only one hydrogen bond (Figure 4D).

As shown in Table II, the effect of the U54–A58 mutations on the aminoacylation kinetics is again complex. The two $tRNA^{Phe}$ mutants U54A and A58G exhibit a slight increase in K_m and less than a 2-fold decrease in k_{cat} resulting in only a 2-fold decrease in k_{cat}/K_m as compared to the wild-type $tRNA^{Phe}$ transcript (Table II). In contrast, the mutant having a C54 is a poor substrate for FRS, showing about a 2-fold increase in K_m and a 5-fold decrease in k_{cat}. All three mutants show reduced rates of lead cleavage. This suggests that despite the relatively simple prediction from model building, mutations of U54 fold improperly thereby reducing binding and reaction with FRS. Alternate base pairing involving this region of *E. coli* $tRNA^{Tyr}$ has been hypothesized to explain the accumulation of precursor in vivo (Reilly & RajBhandary, 1986).

The U8–A14 Tertiary Interaction. A second reverse Hoogsteen tertiary base pair involves the conserved U8 and

A14 nucleotides (Figure 5A). This tertiary base pair is located in the core region of the tRNA and is stacked between the G15–C48 tertiary base pair and the terminal C13–G22 base pair in the D stem (Figure 1) and serves to stabilize the sharp turn in the polynucleotide chain between the acceptor stem and A9. Although many prokaryotic tRNAs have 4-thiouridine at position 8, this modification would not be expected to alter this tertiary base pair. Since U8 is conserved in all tRNAs, a contact between this nucleotide and the synthetase could not be discriminatory but could contribute to the stability of the tRNA synthetase complex. The specific reduction of 4-thiouridine to dihydrouridine in *E. coli* $tRNA^{Tyr}$ results in a loss of aminoacylation activity with its cognate tyrosyl-tRNA synthetase (Starzyk et al., 1985). In addition, Ile-tRNA synthetase is able to catalyze the exchange of ^3H into the 4-thio-U8 of $tRNA^{Ile}$ (Schoemaker & Schimmel, 1976). Starzyk et al. (1982) proposed that a stabilizing Michael adduct is formed between a nucleophile on the synthetase (probably a cysteine) and the C6 of the uridine ring. If a similar interaction occurs between $tRNA^{Phe}$ and FRS, a mutation at this position would be expected to affect the aminoacylation kinetics. Again, due to the reverse Hoogsteen pairing scheme between U8 and A14, nucleotide substitutions at these positions are likely to disrupt this tertiary interaction to some degree. However, by use of the same approach as for the similar U54–A58, three mutants were synthesized U8A, U8C, or A14G. It is important to emphasize that the U8–A14 and U54–A58 reverse Hoogsteen base pairs are located in different regions of the tRNA with different phosphodiester backbone conformations and neighboring bases.

As shown in Table II, the $tRNA^{Phe}$ mutants having either an A8–A14 or a C8–A14 tertiary interaction exhibit a 2-fold increase in K_m and a near normal k_{cat}, resulting in a 2–3-fold decrease in k_{cat}/K_m. While C8 could interact with FRS in a manner similar to that of U8, the structure of A8 is sufficiently different to suggest that FRS does not form a Michael adduct or any other important interaction with U8. The mutant tRNA having a U8–G14 tertiary interaction exhibits a significant increase in K_m resulting in a 5-fold decrease in k_{cat}/K_m. Although this could suggest a possible nondiscriminatory contact between FRS and A14, the lead cleavage rates for all three mutants suggest that the structure in this region of the tRNA has been altered. In addition, close inspection of the yeast $tRNA^{Phe}$ crystal structure reveals that A14 is nearby the known G20 recognition nucleotide. Model building indicates that a guanosine at position 14 would introduce its exocyclic amino functional group into the variable pocket only 5 Å from G20. Thus, it is possible that this amino group prevents proper contact between FRS and G20, resulting in a reduced affinity for the G14 mutant. We therefore suggest that although FRS is sensitive to this region of the tRNA, it most likely does not recognize either U8 or A14 specifically.

The role of the conserved U8–A14 pair has been examined in other systems. Although the U8C mutation reduces the efficiency of the *E. coli* $tRNA^{Ala}$ suppressor (Hou & Schimmel, 1988), it has no apparent effect on the identity of the tRNA. In contrast, mutations in U8 abolish splicing of tRNA precursors in yeast (Reyes & Abelson, 1988) and *Xenopus* (Mattoccia et al., 1988).

The G15–C48 Tertiary Interactions. Levitt (1969) first noted a covariance between the conserved purine at position 15 in the D loop and the conserved pyrimidine at position 48 in the variable loop and proposed that these two nucleotides interact. The crystal structure of yeast $tRNA^{Phe}$ shows a trans base pair between G15 and C48 (Figures 1 and 6A). The

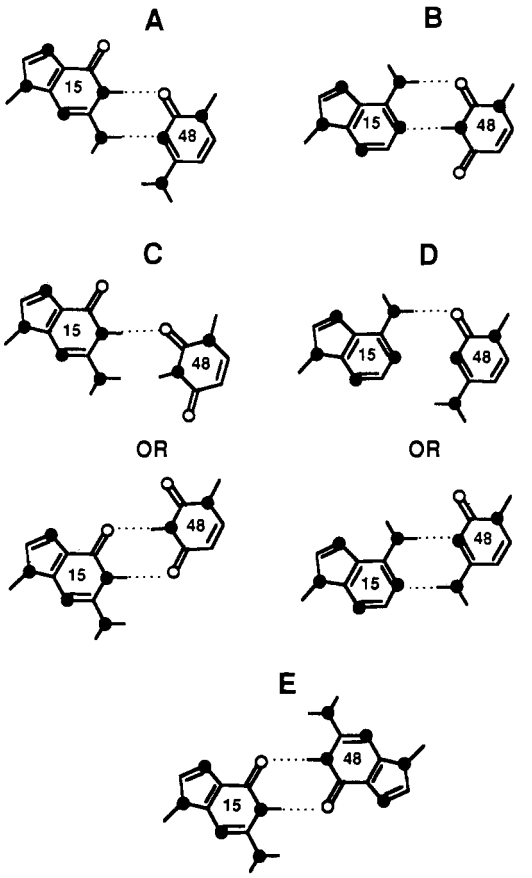

FIGURE 6: Proposed hydrogen bonding for mutations in the semi-conserved G15–C48 pair. (A) G15–C48, (B) A15–U48, (C) G15–U48, (D) A15–C48, and (E) G15–G48.

crystal structure of yeast $tRNA^{Asp}$ reveals a similar trans pair between A15 and U48 which also maintains two hydrogen bonds (Figure 5B; Westhof et al., 1985). However, the difference in the hydrogen-bonding schemes for these alternate tertiary pairs requires a different positioning of the phosphate backbone, resulting in different stacking with the neighboring nucleotides. Model building reveals that with a similar small distortion of the phosphate backbone, both G15–U48 and A15–C48 trans base pairs can form with a single hydrogen bond (Figure 6C,D). Alternatively, by further displacing the phosphate backbone, G15–U48, A15–C48, and even G15–G48 can form a trans pair with two hydrogen bonds.

As shown in Table II, the A15–U48 tRNA exhibits a normal K_m and a greater k_{cat}, resulting in a k_{cat}/K_m 1.5-fold greater than that of the wild-type $tRNA^{Phe}$. The G15A mutant also exhibits a virtually normal K_m and a measurable increase in k_{cat}, whereas the C48U mutant is a slightly poorer substrate due to a 2-fold increase in K_m. In contrast, the C48G is a much poorer substrate having 4-fold decrease in k_{cat}/K_m. The values of k_{cat}/K_m for these four mutant tRNAs correlate with their respective rates of lead cleavage, suggesting that the reduction in aminoacylation rates is primarily due to alterations in the folding of the mutant tRNAs and not due to direct contacts with FRS.

The C13–G22–G46 Tertiary Interaction. The C13–G22 base pair in the D stem interacts with m^7G46 in the variable loop in the core region of the tRNA by forming two hydrogen bonds between the G residues (Figures 1 and 7A). In addition, two base–backbone interactions are also present between the exocyclic amines of G46 and C13 and the phosphate oxygens of P9, which serve to further stabilize the sharp bend between residues 9 and 10. Although the methylation of G46

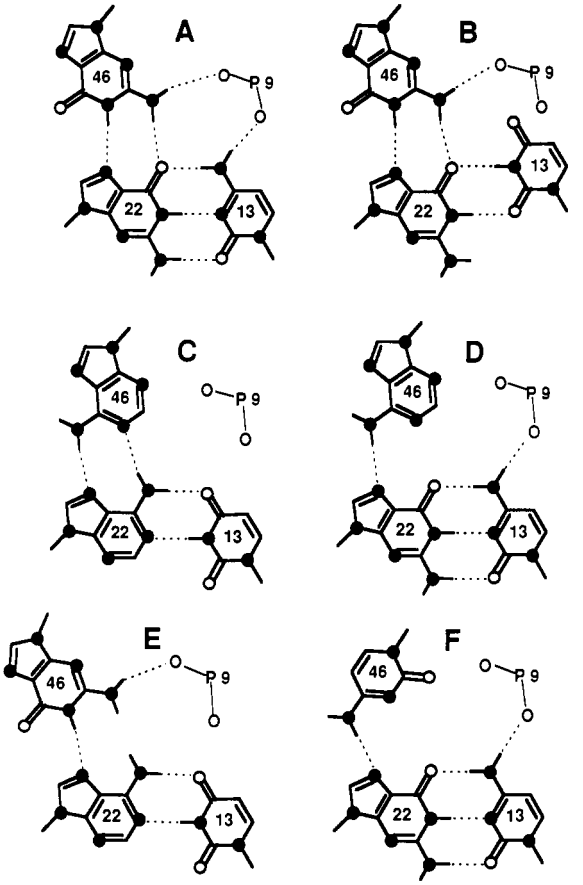

FIGURE 7: Proposed hydrogen bonding for mutations in the semi-conserved C13–G22–m^{7}G46 triple. (A) C13–G22–G46, (B) U13–G22–G46, (C) U13–A22–A46, (D) C13–G22–A46, (E) U13–A22–G46, and (F) C13–G22–C46.

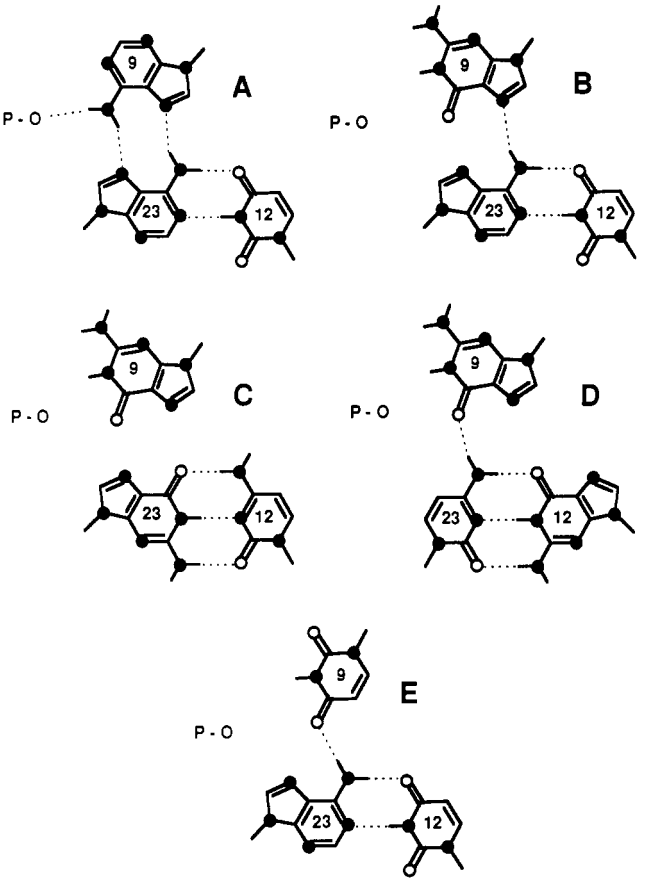

FIGURE 8: Proposed hydrogen bonding for mutations in the semi-conserved (A) A9–A23–U12, (B) G9–A23–U12, (C) G9–A23–U12, (D) G9–C23–G12, and (E) U9–A23–U12.

is not directly involved in the tertiary interaction and is not present in all tRNAs, it could increase the stacking with the adjacent tertiary interactions and thus stabilize the tRNA structure. Of 132 nonmitochondrial tRNAs which have 4 pairs in the D stem about 75% maintain C13–G22–G46, while the remainder have other nucleotides at these positions that are expected to form similar tertiary interactions. The number of hydrogen bonds required to maintain the tertiary interaction can vary. For example, yeast tRNA^{Asp} has a U13–G22–A46 triple with only a hydrogen bond between G22 and A46 and neither of the P9 bonds. It is not even clear that a tertiary interaction between positions 22 and 46 forms for every tRNA. Brennan and Sundaralingam (1976) note that many of the tRNAs which appear to lack the Py13–Pu22 pair in the D stem also lack a plausible 22–46 interaction. Furthermore, the class of tRNAs having a stem–loop structure in the variable region generally include position 46 as a base pair in the stem.

We prepared five mutant tRNAs that all maintain the phylogenetically conserved Py13–Pu22 motif and have different nucleotides at position 46. These include combinations that are found in other tRNAs as well as some that are virtually never found. Model building indicated that with minimal backbone distortions all of the mutants could maintain at least two of the tertiary hydrogen bonds which connect position 46 with the base pair and phosphate 9 with the base triple (Figure 7). All five of these conservative mutants show relatively small differences in their aminoacylation kinetics (Table III). The two mutants having either a U13–G22–G46 or a U13–A22–A46 exhibit a normal K_m and a slight increase in k_{cat}, resulting in a 1.2–1.4-fold increase in k_{cat}/K_m as compared to that of the wild-type tRNA^{Phe} transcript. The mutants having either a C13–G22–A46 or a U13–A22–G46 also exhibit a normal K_m but have reduced k_{cat} values, resulting in a 1.5- and 2-fold decrease in k_{cat}/K_m, respectively. The C46 was the least active with a 2.5-fold decrease in k_{cat}/K_m. It is likely that these small changes in rate are a consequence of the enzyme responding to small alterations in the backbone structure of the transcript. Lead cleavage rates for several of these mutants exhibit similar reduction (Behlen et al., 1990). It is unlikely that FRS contacts any one of the residues specifically; the conservative nature of the mutations leaves open the possibility of a nondiscriminatory contact. For example, the O2 of Py22 in the minor groove of the D stem is present in all mutants tested.

The available evidence suggests that the 13–22–46 base triple is not a site of contact for any tRNA synthetase. Similar conservative mutations in this triple for the amber suppressor tRNA^{Ala} had no effect on the identity or suppressor efficiency of tRNA^{Ala} (Hou & Schimmel, 1988). In several cases among the *E. coli* and yeast tRNAs, variations of the 13–22–46 triple are observed within a group of isoacceptors. Thus, it appears that the role of this tertiary interaction is to help maintain the overall folding of tRNA rather than to serve as a contact for the synthetase.

The A9–A23–U12 Tertiary Interaction. As shown in Figure 8A, A9 forms a reverse Hoogsteen pair with A23 in the major groove of the A23–U12 base pair in the D stem in which two hydrogen-bonding interactions are maintained between A9 and A23. In addition, a single hydrogen bond is formed between the exocyclic amine of A9 and the O2 of phosphate 23. This tertiary interaction is flanked by the C13–G22–G46 and G45–G10–C15 base triples (Figure 1) and thus stabilizes the base stacking of G45 and G46 and the sharp bend between

U8 and A9. The frequently observed G9–C23–G12 triple is found in the *E. coli* $tRNA^{Metf}$ crystal structure (Woo et al., 1980) and is structurally similar to the A9–A23–U12 base triple by maintaining a single hydrogen bond between the exocyclic amine of C23 and the O6 of G9 (Figure 8D) (Kim, 1976). While a vast majority of tRNAs have one of these two base triples, sequence comparison suggests other possibilities (Table I). For example, 4% of the tRNAs have a G9–A23–U12 which could be stabilized by a single hydrogen between the N7 of G9 and the exocyclic amine of A23 (Figure 8B). Although a uridine at position 9 is seldom found, it is possible to form a single tertiary hydrogen bond between the O4 of U9 and the exocyclic amine of A23 (Figure 8F). Finally, 4% of tRNAs have a G9–G23–C12, even though no apparent hydrogen bond can be formed between G9 and G23 (Figure 8C). It was pointed out by Brennan and Sundaralingam (1976) that a G9–G23–C12 triple is a common feature among those tRNAs which are thought to also lack the Py13–Pu22–Pu46 tertiary interaction. Thus, it is possible that the tertiary interaction between A9 and A23 in yeast $tRNA^{Phe}$ is likewise not essential for the proper folding of certain tRNAs.

The aminoacylation kinetic data for the four yeast $tRNA^{Phe}$ mutants having nucleotide substitutions at these positions are given in Table III. The two mutants having either a G9–A23–U12 or G9–G23–C12 tertiary interaction show near normal aminoacylation kinetics, whereas the U9–A23–U12 and G9–C23–G12 mutants exhibit a 2-fold increase in K_m resulting in a 2-fold decrease in k_{cat}/K_m. This strongly suggests that FRS makes no specific contacts with any of these three nucleotides, consistent with the high level of activity observed for *S. pombe* $tRNA^{Phe}$ (McCutchen et al., 1978) and $tRNA^{Arg \rightarrow Phe}$ (Sampson et al., 1989) which have a G9–C23–G12 tertiary interaction. These data further suggest that hydrogen bonds between A9 and both the phosphate and the adenosine at position 23 are not required for FRS recognition. Surprisingly, the G9–G23–C12 mutant, which should disrupt both tertiary hydrogen bonds, is a better substrate than the more phylogenetically conserved and presumably more structurally stable G9–C23–G12 mutant. Perhaps the G9–G23–C12 triple is stabilized by tightly bound water or the extensive stacking between the adjacent C12–G22–G46 and G45–G10–C25 triples.

Like the C13–G22–G46 tertiary interaction, experimental evidence suggests that the identity of the 9–23–12 base triple is also not important for other tRNA synthetase interactions. For example, it was shown that substitution of the 23–12 base pair had no effect on either the identity or the suppression efficiency of an *E. coli* $tRNA^{Ala}$ amber suppressor (Hou & Schimmel, 1988). The two *E. coli* isoacceptor lysyl-tRNAs also have different nucleotides at these three positions.

The G45–G10–C25 Interaction. In this third tertiary interaction involving three nucleotides, the exocyclic amine of G45 in the variable loop forms a single hydrogen bond with the O6 of G10 in the G10–C25 base pair in the D stem (Figure 9A). A unique feature of this base triple is that it is not coplanar. G45 is tilted and stacked over A44, whereas the G10–C25 base pair is stacked over G26. It is evident from the crystal structure that this "twisted" base triple maximizes the stacking between neighboring nucleotides and thus serves to stabilize the coaxial stacking between the anticodon and D stems; 56% of tRNAs have this base triple, and an additional 15% have either U25 or Ψ25, which form a similar base triple involving a G10–U25 wobble base pair in D stem (Figure 9B). While 19% of the tRNAs in this class have a uridine at position 45, which cannot form an obvious tertiary hydrogen bond,

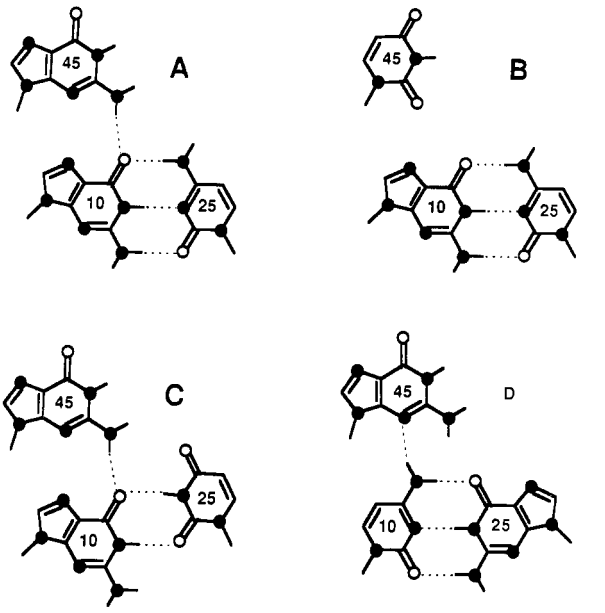

FIGURE 9: Proposed hydrogen bonding for mutations in the semi-conserved G45–m_2G10–C25 triple (A) G45–G10–C25, (B) U45–G10–C25, (C) G45–G10–U45, and (D) G45–C10–G25.

perhaps a tightly bound water molecule could mediate a stable tertiary interaction between U45 and G10. Finally, a G45–C10–G25 base triple is never found in this class of tRNAs but could maintain a similar tertiary hydrogen bond between the N3 of G45 and the exocyclic amine of C10 (Figure 9D).

As shown in Table III, the mutants having either a G45–G10–U25, a U45–G10–C25, or a G45–C10–G25 tertiary interaction exhibit virtually normal aminoacylation kinetics as compared to the wild-type $tRNA^{Phe}$. This strongly suggests that no specific contacts are made between these nucleotides and FRS. The aminoacylation kinetic data for the wild-type *S. pombe* $tRNA^{Phe}$ which has a G45–G10–Ψ25 base triple supports this view. Since three of the mutants were chosen to maintain some pairing potential, it is not possible to comment on the importance of this interaction for maintaining the structure of the tRNA.

The G26–A44 Tertiary Interaction. Yeast $tRNA^{Phe}$ contains a tertiary base pair between m_2^2G26 and A44 at the junction between the dihydro and anticodon stems (Figure 1). The two nucleotides exhibit a propeller-like twisting in which G26 is stacked on the G10–C25 base pair in the D stem and A44 is stacked on the first base pair in the anticodon stem, thereby stabilizing the coaxial stacking between the anticodon and D stems. Although the dimethylamino group on G26 could facilitate the propeller twist (Quigley & Rich, 1976), the crystal structures of yeast $tRNA^{Asp}$ and *E. coli* $tRNA^{Met}$ reveal a similar propeller twist with an unmodified G26 and A44 (Westhof et al., 1985; Woo et al., 1980). Thus, the unmodified $tRNA^{Phe}$ transcript is likely to have a similar pairing geometry (Figure 10A). Although G26–A44 is the most common, a variety of other combinations of nucleotides are found in other tRNAs (Table I). Four mutant tRNAs containing several of these alternate base-pairing interactions were made (Figure 10). Model building suggests that the A26–G44 and G26–U44 pairs would maintain two hydrogen bonds, whereas the A26–A44 pair will have only one hydrogen bond. The tRNA with G26–G44 could also form two hydrogen bonds if one of the guanines adopts a syn conformation. However, with the exception of the A26–G44, some movement of the phosphodiester backbone would be required to accommodate these proposed interactions.

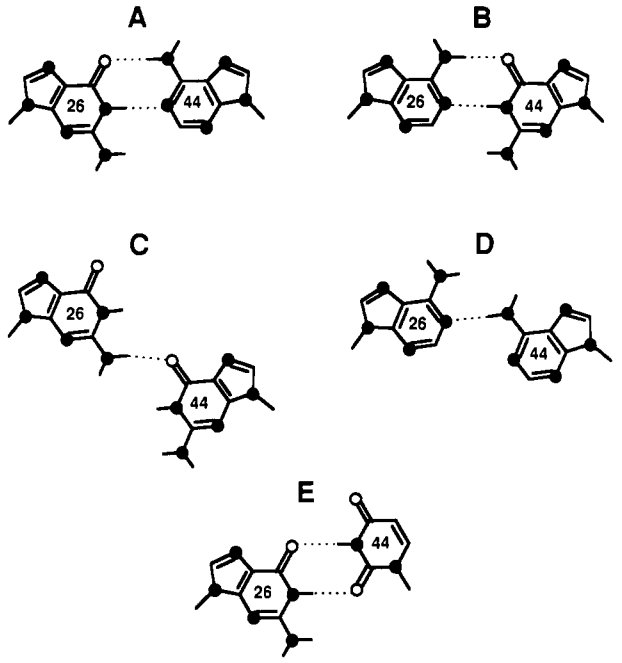

FIGURE 10: Proposed hydrogen bonding for mutation in the semi-conserved m_2^2G26–A44 pair (A) G26–A44, (B) A26–G44, (C) G26–G44, (D) A26–A44, and (E) G26–U44.

All four mutant tRNAs have a slightly lower K_m, resulting in a 1.2–1.6-fold increase in k_{cat}/K_m as compared to that of the wild-type $tRNA^{Phe}$ transcript (Table III). Although not all combinations were tested, it is unlikely that FRS makes specific contact with these nucleotides. It is interesting that these mutants are the only ones tested which decrease the K_m to a value closer to what is observed for the fully modified yeast $tRNA^{Phe}$. Perhaps the alternate base pairs make the conformation of the tRNA transcript resemble native yeast $tRNA^{Phe}$ having a modified G26 residue. Alternately, these mutations may simply relax the structure of the tRNA in this region which facilitates the interaction between the recognition nucleotide and FRS.

In conclusion, we have shown that when many of the tertiary nucleotides were substituted in such a way as to maintain the structure of $tRNA^{Phe}$, little or no change in the aminoacylation kinetics was observed. While not all possible mutations have been made, it is likely that although the tertiary nucleotides may have an important role in the folding of $tRNA^{Phe}$, they do not contact FRS directly. Experiments defining the recognition nucleotides for several other tRNA synthetases reach a similar conclusion. Sequence-specific contacts with tertiary nucleotides have not been implicated for the *E. coli* methionyl, alanyl, seryl, and arginyl enzymes (Schulman & Pelka, 1988; Hou & Schimmel, 1988; Normanly et al., 1986; McClain & Foss, 1988a,b). The only exception is the *E. coli* FRS where A44 and G45 are proposed to contribute to the identity of $tRNA^{Phe}$ (McClain & Foss, 1988c).

Because of the high magnesium ion concentration used in the aminoacylation experiments and the conservative design of the mutations, rather small decreases in k_{cat}/K_m were observed with mutations expected to disrupt the tertiary interaction. Depending on the type of mutation and the location of the tertiary interaction, the k_{cat}/K_m was reduced from 2- to 5-fold. Mutations that disrupted one of the three base triples tended to reduce k_{cat}/K_m less than mutations that disrupted the highly conserved tertiary pairs in the D loop–T loop interaction. This observation is consistent with the proposal of Brennan and Sundaralingam (1976) that the base triples have only a minor role in maintaining the tRNA structure. We have carried out a limited number of aminoacylation experiments on mutant tRNAs at 2 mM $MgCl_2$ where the synthetase is known to be more accurate (Loftfield et al., 1981). The effect of a mutation at the lower magnesium concentration was not always the same as the high magnesium concentration. For the G19C mutation, k_{cat}/K_m was 5-fold less than that of the wild type at both 2 and 15 mM $MgCl_2$. In contrast, the U8C mutation had a k_{cat}/K_m 17-fold lower than that of the wild type at 2 mM $MgCl_2$, whereas the difference was only 3-fold at 15 mM $MgCl_2$. Presumably U8C and G19C mutations affect the folding of tRNA very differently, so that the U8C tRNA can be substantially stabilized by raising the magnesium concentration. It will be interesting to establish the relative contributions of different tertiary interactions and magnesium ion binding to the energetics of tRNA folding.

We have observed several cases in which a successful tertiary interaction could be made with nucleotides seldom found in other tRNAs. For example, we were able to change the completely conserved nucleotides G19, C56, U8, U55, and A58 with little or no effect on aminoacylation. This suggests that the folding geometry of tRNA can be achieved by a much greater variety of sequences than are seen in natural tRNAs. This raises the possibility that a tRNA-like fold could be present in other RNA molecules but difficult to recognize due to the absence of conserved nucleotides. Establishing the sequence requirements for the tRNA fold would therefore aid greatly in RNA structure predictions.

References

Behlen, L. S., Sampson, J. R., DiRenzo, A. B., & Uhlenbeck, O. C. (1990) *Biochemistry* (preceding paper in this issue).

Brennan, T., & Sundaralingam, M. (1976) *Nucleic Acids Res. 3*, 3235–3251.

Brown, R. S., Dewan, J. C., & Klug, A. (1985) *Biochemistry 24*, 4785–4801.

Bruce, G. A., & Uhlenbeck, O. C. (1982) *Biochemistry 21*, 855–861.

Erdmann, V. A., Sprinzl, M., & Pongs, O. (1973) *Biochem. Biophys. Res. Commun. 54*, 942–948.

Grosjean, H., Cedergren, R. J., & McKay, W. (1982) *Biochemie 64*, 387–397.

Hall, K., Sampson, J., Uhlenbeck, O., & Redfield, A. (1989) *Biochemistry 28*, 5794–5801.

Hou, Y. M., & Schimmel, P. (1988) *Nature 333*, 140–145.

Kim, S. H. (1976) *Prog. Nucleic Acid Res. Mol. Biol. 17*, 181–216.

Kim, S., Sussman, J. L., Suddath, F. L., Quigley, G. J., McPherson, A., Wang, A. H., Seeman, N. C., & Rich, A. (1974) *Proc. Natl. Acad. Sci. U.S.A. 71*, 4970–4974.

Klug, A., Ladner, J. E., & Roberts, J. D. (1974) *J. Mol. Biol. 89*, 511–516.

Levitt, M. (1969) *Nature 224*, 759–763.

Loftfield, R. B., Eigner, E. A., & Pastuszyn, A. (1981) *J. Biol. Chem. 256*, 6729–6735.

Mattoccia, E., Baldi, I. M., Gandiwi-Attardi, D., Ciafrè, S., & Tocchini-Valentini, G. P. (1988) *Cell 55*, 731–738.

McClain, W., & Foss, K. (1988a) *Science 240*, 793–796.

McClain, W., & Foss, K. (1988b) *Science 241*, 1804–1807.

McClain, W., & Foss, K. (1988c) *J. Mol. Biol. 202*, 697–709.

McCutchen, T., Silverman, S., Kohli, J., & Soll, D. (1978) *Biochemistry 17*, 1622–1628.

Moras, D., Lorber, B., Romby, P., Ebel, P., & Geige, R. (1983) *J. Biomol. Struct. Dyn. 1*, 209–223.

Morin, G. B., & Cech, T. R. (1988) *Nucleic Acids Res. 16*, 327–346.

Normanly, J., Ogden, R., Horvath, S., & Abelson, J. (1986) *Nature 321*, 213-219.
Quigley, G. J., & Rich, A. (1976) *Science 194*, 796-806.
Reilly, R. M., & RajBhandary, U. L. (1986) *J. Biol. Chem. 261*, 2928-2935.
Reyes, V. M., & Abelson, J. (1988) *Cell 55*, 719-730.
Riesner, D., Pingoud, A., Boehme, D., Peters, F., & Maass, G. (1976) *Eur. J. Biochem. 68*, 71-80.
Rigler, R., Pachmann, U., Hirsh, R., & Zachau, H. G. (1976) *Eur. J. Biochem. 74*, 307-315.
Robertus, J. D., Ladner, J. E., Finch, J. T., Rhodes, D., Brown, R. S., Clark, B. F. C., & Klug, A. (1974) *Nature 25*, 546-551.
Roe, B., Sirover, M., & Dudock, B. (1973) *Biochemistry 12*, 4146-4154.
Romby, P., Moras, D., Bergdoll, M., Dumas, P., Vlassov, V., Westhof, E., Ebel, J. P., & Giegé, R. (1985) *J. Mol. Biol. 184*, 455-471.
Sampson, J. R., & Uhlenbeck, O. C. (1988) *Proc. Natl. Acad. Sci. U.S.A. 85*, 1033-1037.
Sampson, J. R., DiRenzo, A. B., Behlen, L. S., & Uhlenbeck, O. C. (1989) *Science 243*, 1363-1366.
Schevitz, R. W., Padjarny, A., Krishnamachari, N., Hughes, J., & Sigler, P. (1979) *Nature 278*, 188-190.
Schoemaker, H. J., & Schimmel, P. R. (1976) *J. Biol. Chem. 251*, 6823-6830.
Schulamn, L., & Pelka, H. (1988) *Science 242*, 765-767.
Starzyk, R., Koontz, S., & Schimmel, P. (1982) *Nature 298*, 136-140.
Starzyk, R., Schoemaker, H., & Schimmel, P. R. (1985) *Proc. Natl. Acad. Sci. U.S.A. 82*, 339-342.
Westhof, E., Dumas, P., & Moras, D. (1985) *J. Mol. Biol. 184*, 119-145.
Woo, N. H., Roe, B. A., & Rich, A. (1980) *Nature 286*, 346-351.

A Sensitive Genetic Assay for the Detection of Cytosine Deamination: Determination of Rate Constants and the Activation Energy†

Lisa A. Frederico,‡ Thomas A. Kunkel,§ and Barbara Ramsay Shaw*,‡

Department of Chemistry, Duke University, Durham, North Carolina 27706, and Laboratory of Molecular Genetics, National Institute of Environmental Health Sciences, Research Triangle Park, North Carolina 27709

Received August 14, 1989; Revised Manuscript Received October 19, 1989

ABSTRACT: Previously it has not been possible to determine the rate of deamination of cytosine in DNA at 37 °C because this reaction occurs so slowly. We describe here a sensitive genetic assay to measure the rate of cytosine deamination in DNA at a single cytosine residue. The assay is based on reversion of a mutant in the *lacZα* gene coding sequence of bacteriophage M13mp2 and employs *ung*⁻ bacterial strains lacking the enzyme uracil glycosylase. The assay is sufficiently sensitive to allow us to detect, at a given site, a single deamination event occurring with a background frequency as low as 1 in 200 000. With this assay, we determined cytosine deamination rate constants in single-stranded DNA at temperatures ranging from 30 to 90 °C and then calculated that the activation energy for cytosine deamination in single-stranded DNA is 28 ± 1 kcal/mol. At 80 °C, deamination rate constants at six sites varied by less than a factor of 3. At 37 °C, the cytosine deamination rate constants for single- and double-stranded DNA at pH 7.4 are 1×10^{-10} and about 7×10^{-13} per second, respectively. (In other words, the measured half-life for cytosine in single-stranded DNA at 37 °C is ca. 200 years, while in double-stranded DNA it is on the order of 30 000 years.) Thus, cytosine is deaminated ~140-fold more slowly when present in the double helix. These and other data indicate that the rate of deamination is strongly dependent upon DNA structure and the degree of protonation of the cytosine. The data suggest that agents which perturb DNA structure or facilitate direct protonation of cytosine may induce deamination at biologically significant rates. The assay provides a means to directly test the hypothesis.

The integrity of genetic information depends upon the inherent chemical stability of bonds in DNA. Reactions involving deamination of bases, imidazole ring opening, or hydrolysis of phosphodiester or glycosylic bonds can result in mutagenesis, cell transformation, and even cell death (Friedberg, 1984). In particular, deamination of cytosine and 5-methylcytosine in DNA generates the bases uracil and thymine. Replication of these deamination products will produce a C·G → T·A transition mutation (Coulondre et al., 1978; Duncan & Miller, 1980).

Previous analytical methods lacked the sensitivity to determine the rate of deamination of cytosine at 37 °C because this reaction occurs so slowly. Therefore, until now, the spontaneous *rate* of cytosine deamination had been estimated only from chemical measurements of the amount of uracil produced from DNA incubated either at high temperatures (Lindahl & Nyberg, 1974) or at extremes of pH (Wang et al., 1982; Ullman & McCarthy, 1973; Shapiro & Klein, 1966). Our continuing interest in understanding the chemical basis

† Parts of this work were suspported by Grant BC-617 from the American Cancer Society and Grant CA44709 from the NIH to B.R.S. B.R.S. was also supported by a Faculty Development Award from the American Cancer Society.
* Correspondence should be addressed to this author.
‡ Duke University.
§ National Institute of Environmental Health Sciences.

0006-2960/90/0429-2532$02.50/0